ARMY RESEARCH LABORATORY

Rare-earth Doped Gallium Nitride (GaN)—An Innovative Path Toward Area-scalable Solid-state High Energy Lasers Without Thermal Distortion

by Michael Wraback and Mark Dubinskiy

ARL-TR-4794 **April 2009**

NOTICES

Disclaimers

The findings in this report are not to be construed as an official Department of the Army position unless so designated by other authorized documents.

Citation of manufacturer's or trade names does not constitute an official endorsement or approval of the use thereof.

Destroy this report when it is no longer needed. Do not return it to the originator.

Army Research Laboratory
Adelphi, MD 20783-1197

ARL-TR-4794 **April 2009**

Rare-earth Doped Gallium Nitride (GaN)—An Innovative Path Toward Area-scalable Solid-state High Energy Lasers Without Thermal Distortion

Michael Wraback and Mark Dubinskiy
Sensors and Electron Devices Directorate, ARL

REPORT DOCUMENTATION PAGE	Form Approved OMB No. 0704-0188

1. REPORT DATE *(DD-MM-YYYY)*	2. REPORT TYPE	3. DATES COVERED (From - To)
April 2009	Final	December 2007 to December 2008

4. TITLE AND SUBTITLE

Rare-earth Doped Gallium Nitride (GaN)—An Innovative Path Toward Area-scalable Solid-state High Energy Lasers Without Thermal Distortion

5a. CONTRACT NUMBER

5b. GRANT NUMBER

5c. PROGRAM ELEMENT NUMBER

6. AUTHOR(S)

Michael Wraback and Mark Dubinskiy

5d. PROJECT NUMBER

FY08-SED-10

5e. TASK NUMBER

5f. WORK UNIT NUMBER

7. PERFORMING ORGANIZATION NAME(S) AND ADDRESS(ES)

U.S. Army Research Laboratory
ATTN: AMSRD- ARL-SE-EM
2800 Powder Mill Road
Adelphi, MD 20783-1197

8. PERFORMING ORGANIZATION REPORT NUMBER

ARL-TR-4794

9. SPONSORING/MONITORING AGENCY NAME(S) AND ADDRESS(ES)

10. SPONSOR/MONITOR'S ACRONYM(S)

11. SPONSOR/MONITOR'S REPORT NUMBER(S)

12. DISTRIBUTION/AVAILABILITY STATEMENT

Approved for public release; distribution unlimited.

13. SUPPLEMENTARY NOTES

14. ABSTRACT

We have demonstrated, for the first time, in situ neodymium (Nd) doping of gallium nitride GaN by plasma-assisted molecular beam epitaxy (PA-MBE). The Nd doping is controlled by the GaN growth conditions and the Nd effusion cell temperature. The Rutherford backscattering spectroscopy (RBS) and secondary ion mass spectrometry (SIMS) data indicated Nd doping as high as ~8 at. %, with no evidence of phase segregation identified by x-ray diffraction (XRD) for Nd up to ~1 at. %. The Nd incorporation reached a limit while maintaining crystal quality. Strong room-temperature (RT) luminescence corresponded to the three characteristic Nd emission multiplets, with the Stark energy levels resolved by photoluminescence (PL) and photoluminescence excitation (PLE). Although the 4*f* electrons were well shielded from the host material, we were still able to observe weak electron-phonon interactions. Spectral correlation of the multiplets for above (325 nm) and below (836 nm) GaN bandgap excitation implied enhanced substitutional doping at the Ga site. The highest RT PL intensities corresponded to a doping level between 0.1–1 at. %. The enhanced substitutional doping at the Ga site and low optical loss in waveguide structures suggests GaN:Nd with a high enough Nd concentration has significant potential for use in simple, area-scalable, RT, diode-pumped, solid-state high energy lasers (HELs).

15. SUBJECT TERMS

High energy laser, thermal conductivity, GaN, Nd, molecular beam epitaxy, Stark energy level, luminescence

16. SECURITY CLASSIFICATION OF:			17. LIMITATION OF ABSTRACT	18. NUMBER OF PAGES	19a. NAME OF RESPONSIBLE PERSON
a. REPORT	b. ABSTRACT	c. THIS PAGE			Michael Wraback
Unclassified	Unclassified	Unclassified	UU	22	19b. TELEPHONE NUMBER (*Include area code*) (301) 394-1459

Standard Form 298 (Rev. 8/98)
Prescribed by ANSI Std. Z39.18

Contents

List of Figures

Acknowledgments

We would like to thank Eric Readinger for growth and physical characterization of the neodymium (Nd) doped gallium nitride (GaN) and helpful discussions; Grace Metcalfe, Keith Graham, and Larry Merkle for optical characterization and helpful discussions; and John Gruber for theoretical modeling and helpful discussions.

INTENTIONALLY LEFT BLANK.

1. Objective

The objective of this effort was to develop a qualitatively new approach to highly scalable diode-pumped solid-state lasers based on rare-earth (RE) neodymium (Nd^{3+}) doping of gallium nitride (GaN), a high thermal conductivity material. Our goal was to fully eliminate the bottleneck in the heat removal process associated with the low thermal conductivity of the gain medium compared to that of heat-sinking materials.

2. Approach

Laser-based directed energy weapons (DEW) are important components for future Army missile defense systems. The diode-pumped, RE-doped, solid-state laser is a very promising path towards achieving a DEW-sufficient level of average power from a reasonably compact device. Even so, the extreme pump power densities, combined with the inevitable non-radiative losses in the pump-lase process, introduce severe thermal loading in the gain medium. Regardless of the sophistication of the heat removal technique and its efficiency, the gain medium itself is the bottleneck for non-distortive heat removal—due to the low thermal conductivity of known gain media compared to that of heat-sinking materials. The best known laser hosts, e.g., yttrium aluminum garnet (YAG), possess thermal conductivities (10–11 W/(m-K)) that are ~1.5 orders of magnitude lower than those of known heat-sinking materials. In order to eliminate this technical hurdle, an innovative gain medium—with a thermal conductivity on the same order as copper (~390 W/(m-K))—must be engineered.

The approach pursued in this work is based on RE doping of GaN, in particular, Nd^{3+}-doped GaN, with a room temperature (RT) thermal conductivity (131–200 W/(m-K)) 10 to 15 times higher than that of Nd:YAG and 20 to 30 times higher than that of Nd: yttrium lithium fluoride (YLF). RE-doped GaN laser development, if successful, would be a breakthrough toward simple, area-scalable, RT (as opposed to cryogenically cooled) solid-state high energy lasers (HELs) with nearly zero thermal distortions, eliminating the need for sophisticated heat management. After Favennec et al. (*1*) demonstrated a reduction in thermal quenching in erbium (Er)-doped materials with increasing bandgap, interest in wide bandgap semiconductors as host materials expanded. In particular, wurtzite GaN has strong ionic bonds that can enhance the intra-$4f^n$ transition probability in the RE^{3+} ion with substitutional occupation of the Ga site. Light emission from GaN doped with europium (Eu), Er, praseodymium (Pr), thulium (Tm), ytterbium (Yb), Nd, and dysprosium (Dy) has been demonstrated by photoluminescence (PL), electroluminescence (EL), and/or cathodoluminescence (CL) (*2*,*3*). As the RE dopant, Nd is an excellent candidate due to its success in Nd-doped solid-state lasers, which have attained power

levels higher than that from any other four-level material (*4*). Nd has been incorporated into GaN through ion-implantation (*5*) and reactive co-sputtering (*6*). Ion-implantation creates doping profiles and damage effects that often require a post implantation anneal due to the amorphisation of the GaN lattice; however, annealing does not completely recover the damage. In GaN ion implanted with Nd, the majority of Nd^{3+} ions sit on the gallium (Ga) substitutional "site;" however, four other "sites" associated with defects have also been identified (*5*). For reactive co-sputtering of GaN with RE atoms, a post-growth anneal (≥700 °C) in nitrogen is often necessary for PL emission (*7*–*9*).

Although PL (*5*) and EL (*7*) from Nd-doped GaN have been observed, the Stark levels of the 4*f* states have never been resolved, partially due to implantation-related damage of the host material and Nd^{3+} ions occupying multiple sites. In this work, in situ doping of GaN with Nd by plasma-assisted molecular beam epitaxy (PA-MBE) is demonstrated for the first time, with enhanced substantial doping at the Ga site (*10*). This growth technique enables the resolution of the Stark energy levels of the Nd^{3+} ion in GaN by PL and photoluminescence excitation (PLE) spectroscopy. The PLE spectroscopy also enables us to define an optimal pumping wavelength amenable to near infrared (IR) diode laser pumping that limits thermal losses. Since the GaN:Nd layers grown by MBE are thin (2–5 μm), we have designed a guided-wave architecture for edge-pumping the device (which provides the highest level of laser efficiency due to the pump and signal mode confinement within a crystalline-guided structure). The successful implementation of this approach should lead to the development of the first diode-pumped Nd^{3+}:GaN laser.

3. Results

3.1 Growth of Nd-doped GaN by MBE

GaN samples were grown with a fixed growth rate at two temperatures. We varied the Nd cell temperature from 850–1025 °C, and the Ga flux, measured as beam equivalent pressure, from 9.8×10^{-6} to 5.6×10^{-7} torr. The secondary ion mass spectrometry (SIMS) profiling tracks the Ga and Nd signals and assumes the Ga signal is associated with a fully dense stoichiometric GaN film. The average Nd doping concentration, over the bulk of the film thickness, is converted to Nd atomic percent within the GaN matrix. A maximum Nd concentration of ~8 at. % is demonstrated in figure 1 (top).

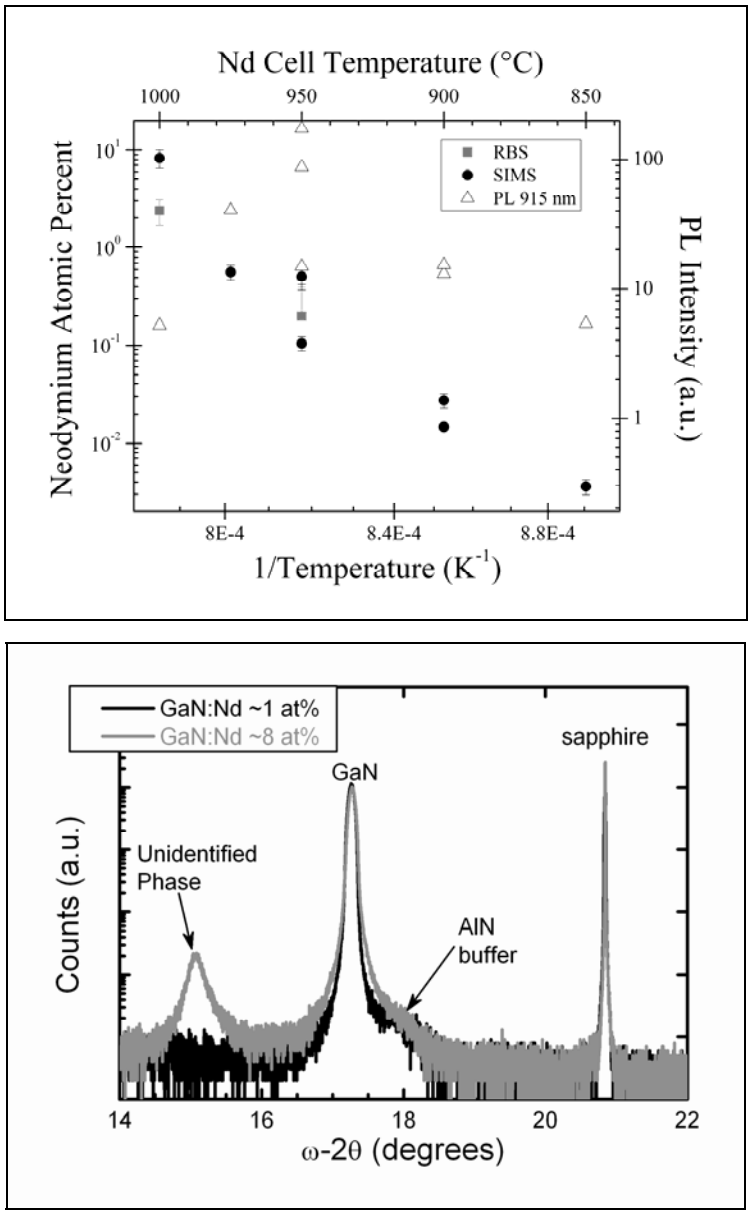

Figure 1. (Top) Nd atomic percent and PL intensity versus Nd cell temperature; (bottom) two x-ray diffraction (XRD) scans of GaN:Nd layers showing the GaN (0002) reflection relative to the sapphire substrate (0006) reflection.

Initial work for incorporating Nd used nitrogen-rich growth, for which the Nd and Ga had little competition for the same lattice site, as excess nitrogen was always present (*10*). These samples produce significant PL intensities of the Nd 4*f* transitions, but only show limited PL output with low Nd atomic percentages and when Nd atomic percentages are greater than 1. The epilayers with high atomic percent Nd (>1) have extra peaks in the XRD data, and the transmission and reflectance data show a diminished intensity, possibly due to Nd clustering or the formation of a second phase. Figure 1 (bottom) also shows typical *ω-2θ* x-ray scans about the (0002) GaN peak

that include the (0006) sapphire peak. The high angle shoulder on the GaN peak (17.27°) is the aluminum nitride (AlN) buffer layer. The typical x-ray rocking curve (XRC) about the GaN (0002) reflection yields a full width at half maximum (FWHM) of ~1400 arcsec, which is consistent with the use of nitrogen-rich growth conditions shown to be favorable for RE optical emission from the GaN matrix (*11*). The FWHM of the XRC data for these nitrogen-rich films implies a high defect density not ideal for thermal properties (*12*). We carried out subsequent growths under varying Ga flux conditions, observing significant improvement under Ga-rich conditions (x-ray data not shown). However, Ga-rich growth potentially leads to less Nd incorporation within the matrix, possibly due to the increased competition for that lattice position.

3.2 Optical Studies of Nd-doped GaN

PL spectra from GaN samples doped with various Nd concentrations showed similar spectral features. Figure 2 shows a typical PL spectrum at low temperature (~30 K) from Nd-doped GaN. Strong emission due to transitions from the $^4F_{3/2}$ excited state to the $^4I_{9/2}$, $^4I_{11/2}$, and $^4I_{13/2}$ manifolds in the energy (wavelength) range 1.30–1.36 eV (910–950 nm), 1.08–1.13 eV (1100–1150 nm), and 0.84–0.89 eV (1400–1480 nm), respectively, are observed. These Nd transitions are redshifted with respect to the same transitions in a Nd:YAG matrix due to the difference in the GaN crystal field. Also, because of the crystal field experienced by substitutional Nd ions at Ga sites, there are a total of J+1/2 Stark sublevels in each manifold, where J is the total angular momentum. The PL peaks appear in pairs separated by 4.1 meV, indicating the splitting energy of the $^4F_{3/2}$ doublet. The most intense emission peaks are observed from transitions to the $^4I_{11/2}$ manifold, with the strongest emission line at 1.12 eV (1106 nm).

Compared to room temperature PL spectra (not shown), the low temperature spectra show relatively small (<1 meV) or no shifts in peak energy position, consistent with the 4*f* shell being well shielded from the host material (*13*). Nonetheless, we observed weak peaks shifted lower in energy from the main peaks by 90 meV, 64 meV, and 11 meV and attributed these to GaN longitudinal optical (LO) photons, transverse optical (TO) phonons, and a RE-related localized mode, respectively. The PL intensity of the 1106 nm peak for direct pumping of the $^4F_{3/2} \rightarrow {}^4I_{9/2}$ transition (915 nm) at room temperature increases with increasing Nd up to ~0.5 at. % (figure 1). At higher Nd concentrations, the decrease in PL intensity may be linked to the diminished transmittance and possibly to quenching associated with the closer proximity of Nd atoms (*14*), as suggested by the additional XRD peak in figure 1. This possibility of quenching is also consistent with the observation of non-exponential fluorescence decay following pulsed excitation. Figure 2 also shows transitions from the $^4I_{9/2}$ ground state to the upper states $^4F_{5/2}$, $^2H_{9/2}$, $^4F_{7/2}$, and $^4S_{3/2}$ between 1.46–1.54 eV (805–850 nm) and 1.58–1.62 eV (765–785 nm), respectively, in the PLE spectra detected at the strongest emission energy 1.12 eV (1106 nm) at low temperature (~13 K). The strongest emission occurs at an excitation energy of 1.48 eV (836 nm). Phonon sidebands shifted higher in energy were also observed in the PLE spectra.

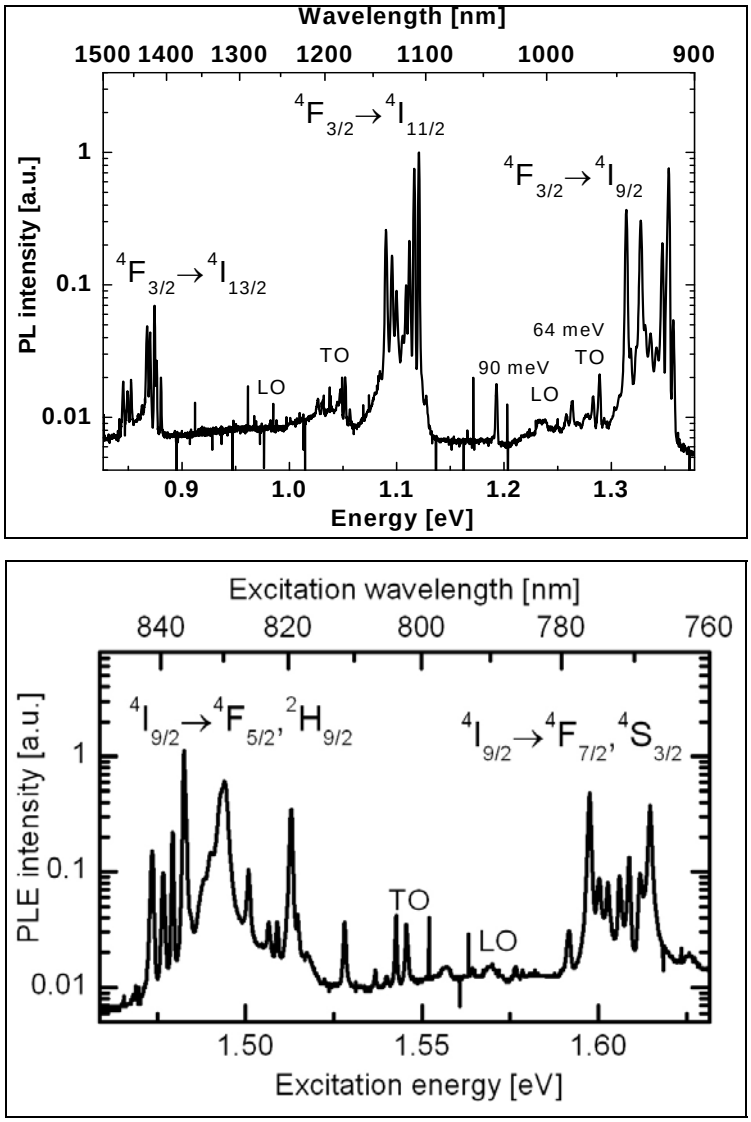

Figure 2. (Top) Low temperature (30 K) PL spectra from GaN:Nd excited at 836 nm; (bottom) PLE spectra from GaN:Nd measured at the 1106 nm emission line at ~13 K.

Figure 3 shows the PL spectra in logarithmic scale from the $^4F_{3/2} \rightarrow {}^4I_{11/2}$ manifold at ~30 K with higher spectral resolution, optically excited below and above the bandgap at 836 nm and 325 nm, respectively. The above bandgap pump creates electrons in the GaN conduction band that relax primarily through non-radiative transitions, presumably through defects, to the upper Nd bands, eventually ending up in the $^4F_{3/2}$ band. In many RE-doped GaN materials, these defects aid in electron transfer to the RE atom, often leading to stronger PL emission from multiple "sites" as described by O'Donnell et al. (*15*). Moreover, when Nd ions occupy multiple sites within the GaN matrix, the PL for above and below bandgap excitation can reveal markedly different spectra. Non-laser-related peaks that only appear in the above bandgap pumping PL are shaded in figure 3. Disregarding the plasma lines, the PL spectra from GaN:Nd excited at 836 nm and

325 nm are nearly identical. These results indicate that the majority of Nd atoms sit on the same "site" within the GaN matrix, with much less influence of defect assisted transitions involving multiple "sites."

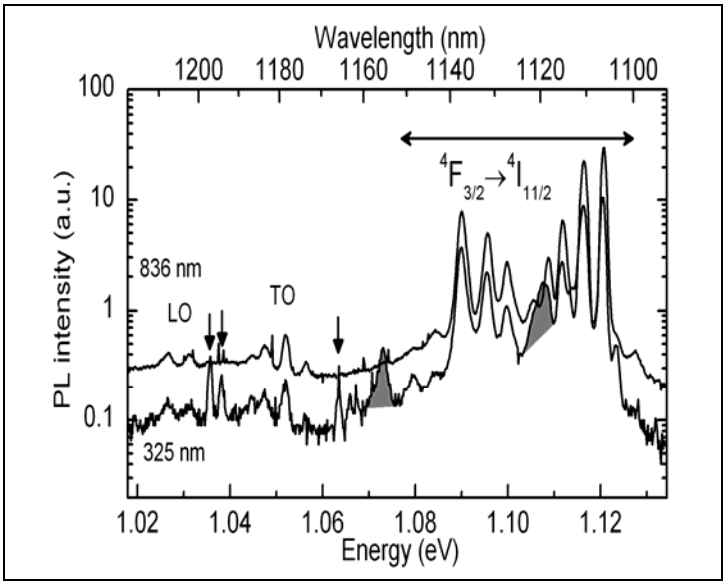

Figure 3. Low temperature (~30 K) photoluminescence spectra from the $^4F_{3/2} \rightarrow {}^4I_{11/2}$ manifold from GaN:Nd optically excited below and above the bandgap at 836 nm and 325 nm, respectively. Peaks marked with a downward arrow indicate plasma lines from the 325 nm laser.

For optical loss and gain measurements, we etched a GaN:Nd sample with a Nd concentration of 0.03 at. % into 750 × 450 μm structures using standard photolithography. We measured the optical loss using the shifting excitation spot (SES) technique (*16*) and the optical gain using the variable stripe length (VSL) method (*17*). Both loss and gain measurements were performed with above bandgap excitation at room temperature. We measured the internal loss coefficient α at the strongest emission energy 1.12 eV (1106 nm). The optical loss is related to the output intensity I by the following equation:

$$I = I_o e^{-\alpha d}, \tag{1}$$

where I_o is the output intensity at the excitation spot and d is the distance between the facet and the excitation spot. A linear fit to $\ln(I/I_o)$ as a function of d gives an optical loss of $\alpha = 6.5 \pm 2$ cm^{-1} (figure 4). This loss is >3 times smaller than that reported for Eu-doped GaN (20 cm^{-1}) at an emission wavelength of 620 nm (*18*).

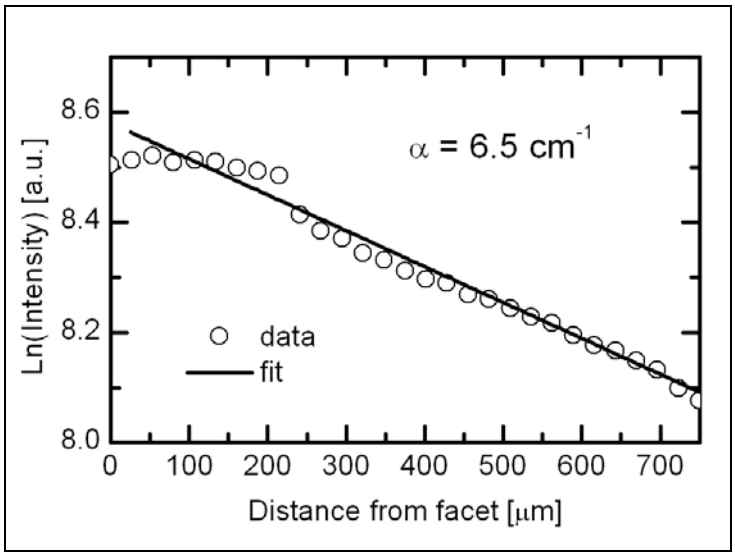

Figure 4. Optical loss at emission energy 1.12 eV (1106 nm) measured using the SES technique; the solid line is a fit of the experimental data (open circles) according to equation 1.

The relationship between output intensity I and net modal gain g_{mod} using the VSL method is given by the following expression:

$$I = \frac{J_o}{g_{mod}}\left(e^{g_{mod}l} - 1\right), \tag{2}$$

where J_o is the spontaneous emission intensity emitted per unit length, l is the length of the excitation beam, and g_{mod} is the net modal gain defined by $g_{mod} = \Gamma g_m - \alpha$. The variables Γ and g_m are the waveguide confinement factor and gain of the material, respectively. Figure 5 shows the output intensity as a function of excitation length. By fitting the experimental data with equation 2, we obtain $g_{mod} = -2 \pm 2$ cm^{-1}, indicating a small gain of the material g_m. The small material gain may be due to the small Nd concentration in the waveguide structure. The discrepancy between the experimental data and the fit in figure 5 at short excitation lengths may be due to effects of the spatial laser intensity profile (*16*).

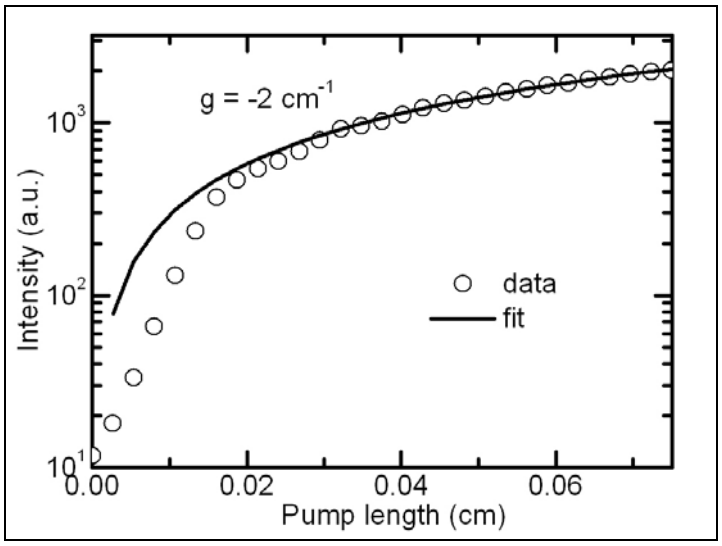

Figure 5. Output intensity versus excitation length measured at emission energy 1.12 eV (1106 nm); the solid line is a fit of the experimental data (open circles) according to equation 2.

4. Conclusions

In conclusion, we have demonstrated, for the first time, in situ Nd doping of GaN by PA-MBE. The Nd doping is controlled by the GaN growth conditions and the Nd effusion cell temperature. The Rutherford backscattering spectroscopy (RBS) and SIMS data indicated Nd doping as high as ~8 at. %, with no evidence of phase segregation identified by XRD for Nd up to ~1 at. %. We found Nd incorporation to reach a limit while maintaining crystal quality. We observed strong RT luminescence corresponding to the three characteristic Nd emission multiplets, with the Stark energy levels resolved by PL and PLE. Although the 4*f* electrons were well shielded from the host material, we were still able to observe weak electron-phonon interactions. Spectral correlation of the three characteristic Nd emission multiplets for above (325 nm) and below (836 nm) GaN bandgap excitation implied enhanced substitutional doping at the Ga site. The highest RT PL intensities corresponded to a doping level between 0.1–1 at. %. The enhanced substitutional doping at the Ga site and low optical loss in waveguide structures suggests GaN:Nd with a high enough Nd concentration has significant potential for use in simple, area-scalable, RT, diode-pumped, solid-state HELs.

5. References

1. Favennec, P. N.; L'Haridon, H.; Salvi, M.; Moutonnet, D.; Leguillou, Y. *Electronic Lett.* **1989**, *25*, 718.
2. Steckl, A. J.; Zavada, J. M. *Mater. Res. Bull.* **1999**, *24*, 16.
3. Steckl, A. J.; Zavada, J. M. *Mater. Res. Bull.* **1999**, *24*, 33.
4. Koechner, W. *Solid-State Laser Engineering*, 5th ed.; Springer, Berlin,1999, p 37.
5. Kim, S.; Rhee, S. J.; Li, X.; Coleman, J. J.; Bishop, S. G. *Phys. Rev.* **1998**, *B57*, 14588.
6. Kim, J. H.; Davidson, M. R.; Holloway, P. H. *Appl. Phys. Lett.* **2003**, *83*, 4746.
7. Kim, J. H.; Holloway, P. H. *Appl. Phys. Lett.* **2004**, *85*, 1689.
8. Kim, J. H.; Holloway, P. H. *J. Appl. Phys.* **2004**, *95*, 4787.
9. Kim, J. H.; Shepard, N.; Davidson, M.; Holloway, P. H. *Appl. Phys. Lett.* **2003**, *83*, 641.
10. Readinger, E. D.; Metcalfe, G. D.; Shen, H.; Wraback, M. *Appl. Phys. Lett.* **2008**, *92*, 061108.
11. Steckl, A. J.; Heikenfeld, J. C.; Lee, D. S.; Garter, M. J.; Baker, C. C.; Wang, Y. Q.; Jones, R. *IEEE J. Sel. Top. Quantum Electron.* **2002**, *8*, 749.
12. Zou, J.; Kutchetkov, D.; Balandin, A. A.; Floresch, D. I.; Pollak, Fred H. *J. Appl. Phys.* **2002**, *92*, 2534.
13. Silkowski, E.; Yeo, Y. K.; Hengehold, R. L.; Goldenberg, B.; Pomrenke, G. S. *Rare Earth Doped Semiconductors II Symposium* **1996**, *69*.
14. Vanuiter, L. G.; Johnson, L. F. *J. Chem. Phys.* **1966**, *44*, 3514.
15. O'Donnell, K. P. ; Hourahine, B. *Eur. Phys. J.-Appl. Phys.* **2006**, *36*, 91.
16. Dal Negro, L.; Bettotti, P.; Cazzanelli, M.; Pacifici, D.; Pavesi, L. *Opts. Commun.* **2004**, *229*, 337.
17. Shaklee, K. L.; Nahory, R. E.; Leheny, R. F. *J. Lumin.* **1973**, *7*, 284.
18. Park, J. H.; Steckl, A. J. *Appl. Phys. Lett.* **2004**, *85*, 4588.

6. Transitions

6.1 Publications: 1

- Readinger, E. D.; Metcalfe, G. D.; Shen, H.; Wraback, M. GaN Doped with Neodymium by Plasma-Assisted Molecular Beam Epitaxy. *Appl. Phys. Lett.* **2008**, *92*, 061108.

6.2 Presentations: 1

- Metcalfe, G. D.; Readinger, E. D.; Shen, H.; Woodward, N. T.; Dierolf, V.; Wraback, M. Energy Levels of Nd^{3+} Ions in GaN. Presented at the International Workshop on Nitride Semiconductors, Montreaux, Switzerland, Oct 2008; Submitted for publication to *Phys. Stat. Sol.*, 2009.

List of Symbols, Abbreviations, and Acronyms

AlN	aluminum nitride
CL	cathodoluminescence
DEW	directed energy weapons
Dy	dysprosium
EL	electroluminescence
Er	erbium
Eu	europium
FWHM	full width at half maximum
Ga	gallium
GaN	gallium nitride
HELs	high energy lasers
IR	infrared
LO	longitudinal optical
Nd	neodymium
PA-MBE	plasma-assisted molecular beam epitaxy
PL	photoluminescence
PLE	photoluminescence excitation
Pr	praseodymium
RE	rare-earth
RBS	Rutherford backscattering spectroscopy
RT	room temperature
SES	shifting excitation spot
SIMS	secondary ion mass spectrometry
Tm	thulium

TO	transverse optical
VSL	variable stripe length
XRC	x-ray rocking curve
XRD	x-ray diffraction
YAG	yttrium aluminum garnet
Yb	ytterbium
YLF	yttrium lithium fluoride

Copies	Organization
1 (PDF only)	DEFENSE TECHNICAL INFORMATION CTR DTIC OCA 8725 JOHN J KINGMAN RD STE 0944 FORT BELVOIR VA 22060-6218
1 CD	DIRECTOR US ARMY RESEARCH LAB IMNE ALC HRR 2800 POWDER MILL RD ADELPHI MD 20783-1197
1 CD	DIRECTOR US ARMY RESEARCH LAB AMSRD ARL CI OK TL 2800 POWDER MILL RD ADELPHI MD 20783-1197
1 CD	DIRECTOR US ARMY RESEARCH LAB AMSRD ARL CI OK PE 2800 POWDER MILL RD ADELPHI MD 20783-1197
3 PDFs	DIRECTOR US ARMY RESEARCH LAB AMSRD ARL SE EM M WRABACK M DUBINSKY L BLISS 2800 POWDER MILL RD ADELPHI MD 20783-1197
ABERDEEN PROVING GROUND	
1 CD	DIR USARL AMSRD ARL CI OK TP (BLDG 4600)
TOTAL:	8 (4 ELEC, 4 CDs)

INTENTIONALLY LEFT BLANK.